Emergence of Crystal-like Atomic Dynamics in Glasses at the Nanometer Scale

G. Baldi,[1,*] M. Zanatta,[2] E. Gilioli,[1] V. Milman,[3] K. Refson,[4] B. Wehinger,[5] B. Winkler,[6] A. Fontana,[7,8] and G. Monaco[5,7]

[1]*CNR-IMEM Institute, Parma Science Park, I-43124 Parma, Italy*
[2]*Physics Department, Perugia University, I-06123 Perugia, Italy*
[3]*Accelrys, 334 Cambridge Science Park, Cambridge CB4 0WN, United Kingdom*
[4]*STFC Rutherford Appleton Laboratory, Chilton, Didcot, Oxfordshire OX11 0QX, United Kingdom*
[5]*European Synchrotron Radiation Facility, BP220, F-38043 Grenoble, France*
[6]*Geowissenschaften, Goethe-Universität, D-60438 Frankfurt a.M., Germany*
[7]*Physics Department, Trento University, I-38123 Povo, Trento, Italy*
[8]*CNR-IPCF, UOS of Roma, c/o Roma University "La Sapienza," I-00185 Roma, Italy*

(Received 12 December 2012; published 1 May 2013)

The vibrational dynamics of a permanently densified silica glass is compared to the one of an α-quartz polycrystal, the silica polymorph of the same density and local structure. The combined use of inelastic x-ray scattering experiments and *ab initio* numerical calculations provides compelling evidence of a transition, in the glass, from the isotropic elastic response at long wavelengths to a microscopic regime as the wavelength decreases below a characteristic length ξ of a few nanometers, corresponding to about 20 interatomic distances. In the microscopic regime the glass vibrations closely resemble those of the polycrystal, with excitations related to the acoustic and optic modes of the crystal. A coherent description of the experimental results is obtained assuming that the elastic modulus of the glass presents spatial heterogeneities of an average size $a \sim \xi/2\pi$.

DOI: 10.1103/PhysRevLett.110.185503 PACS numbers: 63.50.Lm, 62.30.+d, 62.65.+k, 64.70.ph

Amorphous solids lack the long-range translational periodicity of crystalline materials. Nevertheless, their structure presents a residual order on the short and medium ranges [1]. At short distances the structure can be characterized in terms of interatomic distances and bond-angles distribution. The medium-range order extends typically over a length $D \sim 2\pi/\Delta Q_0$ of a few (~ 5) interatomic distances, as indicated by the width ΔQ_0 of the first sharp diffraction peak in the static structure factor, $S(Q)$. The length scale of the nanometer is believed to be the relevant one to understand the phenomenology of the glass transition. In fact, close to the dynamical arrest, the atomic motion of a supercooled liquid is characterized by nanometer-sized regions where the molecules move cooperatively [2–7]. Recent numerical simulation studies [8–10] have also given some evidence of the presence of static correlation lengths of a size comparable to the dynamical correlations, by investigating either subtle structural order parameters [8] or point to set correlations [9,10]. However these quantities are not easily accessible experimentally, because they are not revealed by standard two-points correlation functions, such as the $S(Q)$. Thereby a detailed description of the medium-range order in glasses is still missing.

Only recently, the development of new experimental probes has given some evidence of the presence of atomic regions of nanometric size in a few amorphous materials. Local symmetries in a colloidal suspension have been detected by means of a cross correlation analysis using coherent x rays [11]. Subnanoscale-ordered regions originating from atomic polyhedra have also been detected in a metallic glass employing an electron nanoprobe supported by an *ab initio* molecular dynamics simulation [12]. On a similar glass a wide spatial distribution of the elastic modulus, on the length scale of the nanometer, has been detected by means of atomic force acoustic microscopy [13]. Here we employ an alternative way to gather information on the structure of the canonical network-forming glass of silica, on the spatial scale of the nanometer. Our approach consists in measuring the vibrational dynamics of the glass as a function of the wave vector and comparing the results with those for the corresponding polycrystal, i.e., the crystalline polymorph characterized by the same density and local structure.

In the macroscopic limit, at long wavelengths, a structural glass behaves as a continuum medium and sustains the propagation of elastic waves. The acoustic modes persist up to frequencies of a few terahertz [14], close to and above the frequency, ν_{BP}, of the "boson peak" (BP), the peculiar excess of vibrational states over the $g(\nu) \sim \nu^2$ Debye density of states [15–20]. Below ν_{BP}, the linewidth, Γ, of the excitation, which is proportional to the sound attenuation coefficient, grows with the fourth power of the frequency: $\Gamma \sim \nu^4$ [21–29]. The nature of this strong scattering regime is highly debated in the literature. Two main physical mechanisms have been proposed: (i) the Rayleigh scattering [30] from fluctuations in the density [31] or in the elastic modulus [32,33] of the glass; (ii) a resonant interaction between vibrational soft modes and sound waves, as predicted by the soft potential model [34,35]. The strong scattering law is reproduced also in harmonic models where the atoms vibrate around the sites of a

regular lattice [36] or on the continuum [37] with a random distribution of interatomic force constants and in models where the equilibrium atomic configurations are randomly distributed in space, according to a given pair distribution function [38,39]. The experiments show that the strong scattering regime persists up to ν_{BP}, above which the linewidth follows an approximately quadratic dependence on the frequency [25–29].

In the present Letter the vibrational dynamics of vitreous silica is compared to that of α-quartz, its crystalline polymorph stable at ambient temperature and pressure. The glass was subjected to a process of permanent densification, in order for the two systems to present a similar elastic response in the macroscopic limit. The studied sample had a density $\rho = 2.67(2)$ g/cm^3, very close to that of the crystal [40] (2.649 g/cm^3). The vibrational dynamics of the samples has been probed employing the high-resolution inelastic x-ray scattering technique, combined with an *ab initio* lattice dynamics calculation of α-quartz.

The experiments have been performed at the inelastic x-ray scattering beam lines, ID16 and ID28, at the European Synchrotron Radiation Facility in Grenoble, France. An x-ray beam of 23.7 keV energy is monochromatized using the (12, 12, 12) Bragg reflection of a Si single crystal in backscattering configuration, providing an overall energy resolution of about 1.3 meV. The glass sample was prepared by permanent densification in a large volume press [41]. The hydrostatic high-pressure densification was carried out in a 6/8-type multianvil apparatus (Rockland Research Corporation) of the IMEM-CNR Institute in Parma, Italy. The pressure was first increased at a rate of 1 GPa/hour up to 8 GPa. The sample was then heated at 770 K, before releasing the pressure at a rate of 0.3 GPa/hour. The polycrystal sample consisted of a powder with grains of a few microns, obtained by grinding an α-quartz single crystal (purchased from MaTecK GmbH). The homogeneity of the powder was controlled by x-ray diffraction, measured with a CCD camera during the experiment.

The spectra of the glass were measured at a temperature of 570 K, in order to enhance the inelastic features with respect to the elastic line, while the inelastic x-ray spectra for the powder were acquired at room temperature. The spectra of both the glass and the powder were analyzed using a single- and a multiple-excitations model [42]. The eigenvalues and eigenvectors of the α-quartz dynamical matrix were computed *ab initio* on a uniform grid sampling of the first Brillouin zone, employing density functional perturbation theory as implemented in the CASTEP code [43]. The inelastic x rays scattering spectra for the polycrystal were then computed in the one-phonon approximation (further details on the numerical calculation can be found in the Supplemental Material [42] and in Ref. [44]).

The inelastic component of the spectra at selected momentum-transfer, Q, values is compared to the *ab initio* results in Fig. 1. In the low wave-vector range, $Q < 2$ nm^{-1}, we note that the spectra of the polycrystal are broader than those of the glass. The elastic waves of an amorphous, isotropic solid in the limit of large wavelengths (low Qs) have a well-defined polarization, either transverse or longitudinal. In this limit only a single peak, associated to the longitudinal wave, has a nonvanishing x-ray scattering cross section. On the contrary, for a single crystal this holds true only along a few high-symmetry directions. In the investigated regime, where the wavelength ($\lambda < 10$ nm) is much smaller than the crystallite sizes (a few microns),

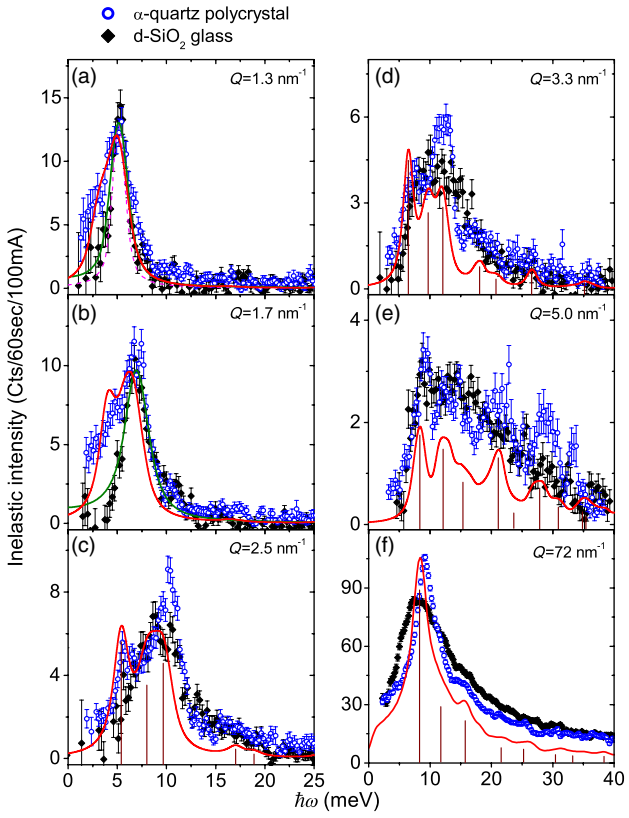

FIG. 1 (color online). The intensity of the x rays inelastically scattered by the α-quartz polycrystalline powder (open blue circles) and by the permanently densified SiO_2 glass (full black diamonds) is shown on the energy loss (Stokes) side at room temperature. The spectra of the glass are properly normalized, taking into account the Bose population factor for phonons to ensure a one to one comparison between the glass and the polycrystal, without any adjustable parameter. The spectra for the polycrystal obtained from the *ab initio* lattice dynamics calculation at the specified wave vectors are plotted as thick red lines. The vertical lines show the main position and intensity of specific single-crystal branches and polarizations, the three acoustic modes corresponding to the lowest energy ones. The green line in panels (a) and (b) is the fit of the glass spectra to a damped harmonic oscillation (DHO) function convoluted with the instrumental resolution function [dashed pink line in panel (a)]. The red curve in panel (f) is the reduced density of vibrational states of the numerical calculation for the crystal, convoluted with the experimental resolution function.

the effects of the single crystal grains boundaries can be neglected and the intensity scattered by the polycrystalline powder, I^{poly}, can be approximated by averaging the single crystal one, I^{cr}, over the wave-vector orientations,

$$I^{\mathrm{poly}}(Q,\hbar\omega) = \frac{1}{4\pi}\int_0^{2\pi} d\phi \int_0^{\pi} d\theta \sin(\theta) I^{\mathrm{cr}}(\bar{Q},\hbar\omega). \quad (1)$$

Here ϕ and θ specify the crystal wave-vector direction and Q its modulus. Because of the directional average, the intensity scattered by the polycrystal powder can thus present a non-negligible component arising from quasi-transverse modes. In fact, the measured spectra of the polycrystal present a quasitransverse excitation whose intensity is comparable to that of the quasilongitudinal one in the entire explored wave-vector range ($Q > 1$ nm^{-1}). The weight of this additional component is much higher than expected from a simple extrapolation from the macroscopic limit [45]. The presence of an important quasitransverse contribution to the spectrum is confirmed by the *ab initio* numerical study, which shows that both transverse modes contribute to $I^{\mathrm{poly}}(Q,\hbar\omega)$ already at the lowest investigated momentum transfers. At higher wave vectors the polycrystal and the glass spectra become very similar, as observed also for ethanol [46], and present contributions from both acoustic and optic modes.

The inelastic component of the spectra has been fitted to a single-excitation model, a DHO function, in order to estimate its linewidth, Γ. The linewidths of the two systems are very similar above a crossover momentum-transfer $Q_c \sim 2$ nm^{-1}, as shown in Fig. 2. The small difference at high Qs has to be ascribed to the inadequacy of a single excitation fit in this regime, as the spectra are almost indistinguishable (see Fig. 1). In this range the spectral width follows approximately a Q^2 law. In the other limit, $Q < Q_c$, the broadening of the spectra of the polycrystal has a linear Q dependence, as expected from the linear region of the dispersion curves. On the contrary, the sound attenuation of the glass shows the strong scattering regime, $\Gamma \sim Q^4$, as found in previous studies [22–27]. Furthermore, the linewidth of the glass in this regime is smaller than that of the polycrystal, as already noted from the inspection of Fig. 1.

The polycrystal excitations disperse up to a Q value of about 6 nm^{-1}, above which all the modes show only minor oscillations around constant values, as shown in Fig. 3. In the figure we plot the map of the measured glass spectral intensity in the energy—wave-vector space, together with the peak positions and the results of the calculations for the polycrystal. The crystal spectrum in the high Q limit, where it is proportional to the reduced vibrational density of states $g(\hbar\omega)/(\hbar\omega)^2$, is dominated by a pronounced peak around 9 meV, arising from the lower transverse acoustic mode at the zone boundary. This feature, the first van Hove singularity, is located very close to the energy, $\hbar\omega_{\mathrm{BP}}$, of the BP in the glass at this density, as shown in panel (f) of Fig. 1. The vibrational modes of the glass are affected by

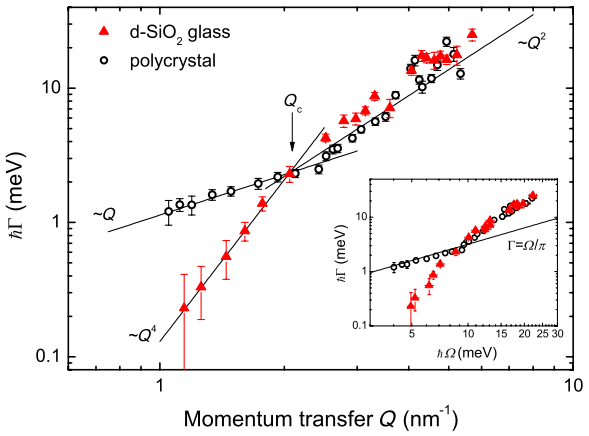

FIG. 2 (color online). The broadening, $\hbar\Gamma$, of the permanently densified SiO_2 glass (red triangles) and of the polycrystal (open black circles) spectra, is plotted as a function of the momentum transfer Q. The lines are guides to the eyes, showing the indicated slopes. The vertical arrow indicates the crossover momentum transfer Q_c. Inset: Inelastic broadening, $\hbar\Gamma$, as a function of the DHO peak position $\hbar\Omega$. The line indicates the IR limit, reached when the amplitude mean free path equals the wavelength, corresponding to the condition: $\Gamma \sim \Omega/\pi$. In the low wave-vector range, $Q < Q_c$, the broadening of the polycrystal spectrum is close to the IR limit because of the relevant spectral weight of the quasitransverse acoustic component, which is absent in the glass spectra in this region.

the absence of translational periodicity, with the consequence that the spectrum of the glass is broader than that of the polycrystal because its zone boundary is not sharply defined. From the ratio between the first sharp diffraction peak width and its position, $\Delta Q_0/Q_0 \sim 0.35$, we can estimate this contribution as a further broadening $\hbar\Delta\omega_{\mathrm{BP}} \sim \hbar\omega_{\mathrm{BP}}\Delta Q_0/Q_0 \sim 3$ meV, in good agreement with the experimental data.

The crossover wave-vector Q_c marks the transition from the long wavelengths regime, where the glass behaves as an isotropic elastic medium, to a microscopic regime where the dispersion curves of the glass are similar to those of the polycrystal, with excitations related to the acoustic and optic modes of the single crystal, as shown by the selection of spectra in Fig. 1 and by the color map in Fig. 3. In this regime the glass spectrum closely resembles that of the polycrystal, I^{poly} (Eq. (1)), apart from being smoother because of the wave-vector uncertainty, ΔQ, associated to the limited extent of structural order [47]. More precisely, the Q-resolved vibrations for the glass arise from the linear combination of the limited subset of the crystal eigenstates whose wave-vectors have a magnitude $|\bar{Q}| = Q \pm \Delta Q/2$. The transition between the two regimes takes place when the probed wavelength crosses the length $\xi \sim 2\pi/Q_c \sim 3$ nm, corresponding to about 20 interatomic distances. This length matches the size of the characteristic structures appearing in the nonaffine displacement field of Lennard-Jones glasses and of silica, as found in numerical simulation studies [48]. The size of

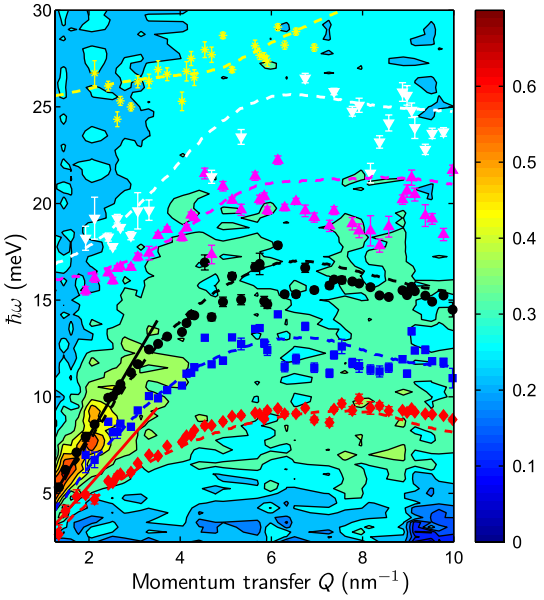

FIG. 3 (color online). The color map of the experimentally determined inelastic intensity of the glass is plotted in the energy ($\hbar\omega$) momentum (Q) space. The color bar is in counts/s/100 mA units. The dispersion curves of the six lower energy branches of the polycrystal are shown as full symbols. The dashed lines are the polycrystal dispersion curves as obtained from the lattice dynamics calculation. The continuum lines are linear dispersions corresponding to the longitudinal and transverse sound velocities expected for the polycrystal in the macroscopic limit from the elasticity theory.

these structures corresponds to the smaller length down to which the continuum elasticity theory is able to describe the response of the glass to a small deformation.

The much-debated Ioffe-Regel (IR) limit [24], defined by the condition that the wave amplitude mean free path equals its wavelength, is also reached at Q_c, as shown in the inset of Fig. 2, where $\hbar\Gamma$ is plotted as a function of the peak energy. The comparison with the polycrystal dynamics provides a simple explanation for this apparent coincidence, because the linewidth of the polycrystal satisfies the IR condition in the entire range below Q_c. At $Q \sim Q_c$ the glass dynamics begins to resemble to that of the corresponding polycrystal and the peak in the glass spectrum acquires contributions from the transverse modes so that it cannot be considered any more as the Fourier transform of a single, albeit attenuated, sound wave. The Q^2 dependence of the linewidth at higher Qs originates from the increase of the intensity of the optic modes with increasing Q, as shown in Fig. 1. The intensity of the optic modes grow faster than that of the acoustic excitations in this Q range, with the effect of a change in slope of the linewidth of both the polycrystal and the glass. A close examination of the Q dependence of the intensity of the vibrational branches can be found in the Supplemental Material [42].

The wave-vector Q_c can be estimated as the point where the sound damping of the glass shows the crossover from the $\sim Q^4$ to the $\sim Q^2$ dependence. For the case of vitreous silica at normal density and ambient conditions, the crossover is located at a Q value about a factor two smaller than for the d-SiO_2 glass here studied [26], leading to a length $\xi \sim 6$ nm. On the contrary, the extension, $D \sim 1$ nm, of the medium range order, estimated from the width of the first diffraction peak in the $S(Q)$, is not affected appreciably by the permanent densification of the glass [49]. The strong dependence of ξ on the density suggests the presence of elastic heterogeneities in the glass, whose average size is markedly affected by the densification process. The existence of elastic heterogeneities with a size $a \sim 1/Q_c \sim \xi/2\pi$ can justify the $\Gamma = AQ^4$ increase of the sound attenuation as arising from the Rayleigh scattering [30–33] of the long- wavelength sound waves from the elastic modulus fluctuations between these domains [50]. Moreover, the marked density dependence of the coefficient A [27], finds in this way a natural explanation in terms of the density dependence of ξ.

In summary, we have shown that the elastic response of a glass is similar to that of an assembly of small anisotropic clusters of a size $a \sim \xi/2\pi$ of the order of the nanometer. The glass vibrations vary from the plane waves of a continuum isotropic elastic body to the excitations of the corresponding crystalline powder, as the wavelength gets smaller than ξ. At these lengths the spectrum of the glass presents typical features of anisotropic systems, like transverse and opticlike modes. It is suggestive to observe that the size of the elastic heterogeneities closely matches the typical sizes of the dynamic heterogeneities in the proximity of the glass transition, which are found in the range 1–3 nm and present a faint increase with the system fragility [3–5,7]. This correspondence can be qualitatively explained by the fact that the atomic mobility in the supercooled liquid is expected to be related to the elastic modulus of the cluster that included the concerned atom in the glass phase.

The authors acknowledge E. Borissenko, V. M. Giordano, and M. Krisch for excellent support and helpful suggestions during the experiments, A. Bosak for discussions and suggestions on the numerical calculations, and S. Caponi and A. Chumakov for useful discussions and comments. G. B. acknowledges the colleagues of the Physics Department of Parma University for many valuable discussions.

*giacomo.baldi@cnr.it

[1] S. R. Elliott, Nature (London) **354**, 445 (1991).
[2] G. Adam and J. H. Gibbs, J. Chem. Phys. **43**, 139 (1965).
[3] U. Tracht, M. Wilhelm, A. Heuer, H. Feng, K. Schmidt-Rohr, and H. W. Spiess, Phys. Rev. Lett. **81**, 2727 (1998).
[4] L. Berthier, G. Biroli, J.-P. Bouchaud, L. Cipelletti, D. El Masri, D. L'Hôte, F. Ladieu, and M. Pierno, Science **310**, 1797 (2005).

[5] C. Crauste-Thibierge, C. Brun, F. Ladieu, D. L'Hôte, G. Biroli, and J.-P. Bouchaud, Phys. Rev. Lett. **104**, 165703 (2010).

[6] L. Berthier and G. Biroli, Rev. Mod. Phys. **83**, 587 (2011).

[7] R. Richert, N. Israeloff, C. Alba-Simionesco, F. Ladieu, and D. L'Hôte, in *Dynamical Heterogeneities in Glasses, Colloids and Granular Media*, edited by L. Berthier, G. Biroli, J.-P. Bouchaud, L. Cipelletti, and W. van Saarloos (Oxford University Press, Oxford, England, 2011).

[8] H. Tanaka, T. Kawasaki, H. Shintani, and K. Watanabe, Nat. Mater. **9**, 324 (2010).

[9] G. Biroli, J.-P. Bouchaud, A. Cavagna, T. S. Grigera, and P. Verrocchio, Nat. Phys. **4**, 771 (2008).

[10] W. Kob, S. Roldàn-Vargas, and L. Berthier, Nat. Phys. **8**, 164 (2012).

[11] P. Wochner, C. Gutt, T. Autenrieth, T. Demmer, V. Bugaev, A. D. Ortiz, A. Duri, F. Zontone, G. Grübel, and H. Dosch, Proc. Natl. Acad. Sci. U.S.A. **106**, 11 511 (2009).

[12] A. Hirata, P. Guan, T. Fujita, Y. Hirotsu, A. Inoue, A. R. Yavari, T. Sakurai, and M. Chen, Nat. Mater. **10**, 28 (2011).

[13] H. Wagner, D. Bedorf, S. Küchemann, M. Schwabe, B. Zhang, W. Arnold, and K. Samwer, Nat. Mater. **10**, 439 (2011).

[14] F. Sette, M. H. Krisch, C. Masciovecchio, G. Ruocco, and G. Monaco, Science **280**, 1550 (1998).

[15] U. Buchenau, N. Nücker, and A. J. Dianoux, Phys. Rev. Lett. **53**, 2316 (1984).

[16] A. P. Sokolov, A. Kisliuk, M. Soltwisch, and D. Quitmann, Phys. Rev. Lett. **69**, 1540 (1992).

[17] A. P. Sokolov, R. Calemczuk, B. Salce, A. Kisliuk, D. Quitmann, and E. Duval, Phys. Rev. Lett. **78**, 2405 (1997).

[18] A. Fontana, R. Dell'Anna, M. Montagna, F. Rossi, G. Viliani, G. Ruocco, M. Sampoli, U. Buchenau, and A. Wischnewski, Europhys. Lett. **47**, 56 (1999).

[19] L. E. Bove, C. Petrillo, A. Fontana, and A. P. Sokolov, J. Chem. Phys. **128**, 184502 (2008).

[20] A. I. Chumakov, G. Monaco, A. Monaco, W. A. Crichton, A. Bosak, R. Rüffer, A. Meyer, F. Kargl, L. Comez, D. Fioretto, H. Giefers, S. Roitsch, G. Wortmann, M. H. Manghnani, A. Hushur, Q. Williams, J. Balogh, K. Parliński, P. Jochym, and P. Piekarz, Phys. Rev. Lett. **106**, 225501 (2011).

[21] W. Dietsche and H. Kinder, Phys. Rev. Lett. **43**, 1413 (1979).

[22] M. Foret, R. Vacher, E. Courtens, and G. Monaco, Phys. Rev. B **66**, 024204 (2002).

[23] B. Rufflé, M. Foret, E. Courtens, R. Vacher, and G. Monaco, Phys. Rev. Lett. **90**, 095502 (2003).

[24] B. Rufflé, G. Guimbretière, E. Courtens, R. Vacher, and G. Monaco, Phys. Rev. Lett. **96**, 045502 (2006).

[25] G. Baldi, V. M. Giordano, G. Monaco, and B. Ruta, Phys. Rev. Lett. **104**, 195501 (2010).

[26] G. Baldi, V. M. Giordano, and G. Monaco, Phys. Rev. B **83**, 174203 (2011).

[27] G. Baldi, V. M. Giordano, G. Monaco, and B. Ruta, J. Non-Cryst. Solids **357**, 538 (2011).

[28] G. Monaco and V. M. Giordano, Proc. Natl. Acad. Sci. U.S.A. **106**, 3659 (2009).

[29] B. Ruta, G. Baldi, V. M. Giordano, L. Orsingher, S. Rols, F. Scarponi, and G. Monaco, J. Chem. Phys. **133**, 041101 (2010).

[30] J. W. S. Rayleigh, *The Theory of Sound* (The Macmillan Company, New York, 1896).

[31] S. R. Elliott, Europhys. Lett. **19**, 201 (1992).

[32] J. E. Graebner, B. Golding, and L. C. Allen, Phys. Rev. B **34**, 5696 (1986).

[33] J. Kawahara, Wave Motion **48**, 290 (2011).

[34] U. Buchenau, Yu. M. Galperin, V. L. Gurevich, D. A. Parshin, M. A. Ramos, and H. R. Schober, Phys. Rev. B **46**, 2798 (1992).

[35] B. Rufflé, D. A. Parshin, E. Courtens, and R. Vacher, Phys. Rev. Lett. **100**, 015501 (2008).

[36] W. Schirmacher, G. Diezemann, and C. Ganter, Phys. Rev. Lett. **81**, 136 (1998).

[37] W. Schirmacher, Europhys. Lett. **73**, 892 (2006).

[38] T. S. Grigera, V. Martín-Mayor, G. Parisi, and P. Verrocchio, Phys. Rev. Lett. **87**, 085502 (2001).

[39] C. Ganter and W. Schirmacher, Phys. Rev. B **82**, 094205 (2010).

[40] R. B. Sosman, *The Properties of Silica* (The Chemical Catalog Company, Inc., New York, 1927).

[41] M. Zanatta, G. Baldi, S. Caponi, A. Fontana, E. Gilioli, M. Krisch, C. Masciovecchio, G. Monaco, L. Orsingher, F. Rossi, G. Ruocco, and R. Verbeni, Phys. Rev. B **81**, 212201 (2010).

[42] See Supplemental Material at http://link.aps.org/supplemental/10.1103/PhysRevLett.110.185503 for further details on the data analysis.

[43] S. J. Clark, M. D. Segall, C. J. Pickard, P. J. Hasnip, M. J. Probert, K. Refson, and M. C. Payne, Z. Kristallogr. **220**, 567 (2005).

[44] A. Bosak, M. Krisch, D. Chernyshov, B. Winkler, V. Milman, K. Refson, and C. Schulze-Briese, Z. Kristallogr. **227**, 84 (2012).

[45] A. Bosak, M. Krisch, I. Fischer, S. Huotari, and G. Monaco, Phys. Rev. B **75**, 064106 (2007).

[46] A. Matic, C. Masciovecchio, D. Engberg, G. Monaco, L. Börjesson, S. C. Santucci, and R. Verbeni, Phys. Rev. Lett. **93**, 145502 (2004).

[47] V. M. Giordano and G. Monaco, Proc. Natl. Acad. Sci. U.S.A. **107**, 21985 (2010).

[48] F. Lèonforte, A. Tanguy, J. P. Wittmer, and J.-L. Barrat, Phys. Rev. Lett. **97**, 055501 (2006).

[49] Y. Inamura, M. Arai, N. Kitamura, S. M. Bennington, and A. C. Hannon, Physica (Amsterdam) **241-243**, 903 (1998).

[50] The average size of the heterogeneities is determined by the condition $aQ_c \sim 1$. This relation defines the maximum wave vector at which the sound attenuation follows the Rayleigh scattering law, as shown in Ref. [33] and references therein.